



A study of hydrogeochemical processes using integrated geochemical and multivariate statistical methods and health risk assessment of groundwater in Trans-Varuna region, Uttar Pradesh

Sughosh Madhav¹ · N. Janardhana Raju¹ · Arif Ahamad¹

Received: 15 March 2019 / Accepted: 3 August 2020 / Published online: 9 August 2020
© Springer Nature B.V. 2020

Abstract

In the current study, 62 groundwater samples were collected (31 each in premonsoon and postmonsoon seasons) and analyzed for various physicochemical parameters and trace metals in the Trans-Varuna region, Uttar Pradesh. From the cationic fields of piper chart, it is viewed that 78% and 81% samples in premonsoon and postmonsoon, respectively, fall in no dominance type, while all the samples in postmonsoon and 97% samples in premonsoon fall in bicarbonate type in anionic facies. The Ca/Mg ratio with an average of 1.44 and 1.15 in pre-monsoon and post-monsoon correspondingly points out that carbonate dissolution is the leading cause of Ca in the Trans-Varuna region. A plot between $[(Na + K) - Cl]$ and $[(Ca + Mg) - (HCO_3 - SO_4)]$ suggests that ion exchange also add ions in the groundwater. According to the Gibbs plot, the hydrogeochemistry of samples signifies that most of the samples are from rock dominance. Saturation indices point out that the groundwater of the Trans-Varuna region is saturated with chalcedony, goethite, hematite, and quartz and undersaturated with reference to anhydrite, aragonite, gypsum, halite, and fluorite. 36% sample in premonsoon and 52% samples in postmonsoon shows high NO_3 concentration which is above the WHO standard for drinking purpose. In terms of Fe, 74% of samples are beyond the permissible limit of WHO. Various indices to estimate the aptness of groundwater for agricultural function indicate that most of the samples in both the seasons are safe of farming uses. Chronic daily intake values show that infants and children of the investigative region are very vulnerable to nitrate contamination. Target health quotient of heavy metals was established in the sequence of $Pb > Zn > Mn > Fe > Ni > Cu$.

Keywords Groundwater · Hydrogeochemical process · Statistical analysis · CDI · THQ · Irrigation

✉ N. Janardhana Raju
rajunj7@gmail.com

¹ School of Environmental Sciences, Jawaharlal Nehru University, New Delhi 110067, India

1 Introduction

It is essential to recognize the evolution of the hydrogeochemical process and geochemical features of groundwater for its sustainable development and effective groundwater management (Chandran et al. 2017). Groundwater quality of any area is functions of physicochemical factors that are significantly governed by geological configurations and human conduct (Madhav et al. 2018a). Fundamental aspects which have direct over water composition incorporate rainfall model and quantity, geological characters of basin and aquifer, climatic features and several water–rock interface procedures in the subsurface environment (Elangovan et al. 2017). Saturation states of water bodies with surrounding rock and minerals also controls the hydrogeochemical processes and water quality of the aquifer (Todd 1980; Hem 1991; Raju et al. 2016). Feldspar and carbonate are the most abundant minerals found in the earth crust, so these minerals are very important for the regulation of the natural water chemistry (Kenoyer and Bowser 1992). The dissolution rate of carbonates such as calcite and dolomite are very high, so these minerals greatly influence the water chemistry (Kim et al. 2004). Hydrogeochemical processes which control the groundwater quality depend on topography and land use of the basin (Chkirbene et al. 2009; Kibena et al. 2014).

Human conducts which manipulate the water composition comprise management of domestic and industrial effluents and mining and farming actions (Arnade 1999; Singh et al. 2016). Groundwater, on the one hand, supports an array of human activities such as drinking, domestic use, agriculture use, and on the other hand, plays a vital role in biogeochemical reactions (Hancock et al. 2005; Huang et al. 2013). Hydrogeochemical features and groundwater pollution in various basins that resulted due to human interference mostly by farming conduct and manufacturing and household effluent have been studied by many researchers (Patel et al. 2016; Thakur et al. 2018).

Multivariate statistical analysis such as correlation matrix, factor examination, and cluster investigation is used to better understand of pollution source and contribution of anthropogenic activities in the contamination (Jeevanandam et al. 2012; Hamzah et al. 2017; Madhav et al. 2018a). The primary purpose of factor analysis is the reduction and summarization of data. Factor analysis may assist in categorizing the original data by generates the general relationship among measured chemical variables (Lu et al. 2011). Polluted water can impose several health risks by diverse routes of disclosure, like water ingestion and through dermal contact. The United State of Environmental Protection Agency (USEPA) has set up significant indices used for human health assessment are Chronic Daily Intake, Hazard Quotient, and Health Risk Index (USEPA 1986; Wu and Sun 2016; Qasemi et al. 2018 Miri et al. 2018).

The dependence of the whole region on groundwater is the crucial region following the selection of this specific region. Land use is a primary factor causing poor water quality. Another reason to choose this area is its intricate land-use pattern. A relatively small area shows different land-use patterns. In the current study, an endeavor has been made to understand the hydrogeological processes using geochemical relations and multivariate statistical analysis to recognize the impacts of natural and human conducts on groundwater composition. Evaluation of groundwater excellence catalogues for the fitness of water for human consumption and farming conduct is included in this study. Human health hazard originated by nitrate, and various heavy metals are also studied in current work.

2 Study area

2.1 Site description

The Trans-Varuna region is placed between the latitude $25^{\circ}15'0''\text{N}$ – $25^{\circ}27'22''\text{N}$ and longitude $82^{\circ}55'00''\text{E}$ – $83^{\circ}06'10''\text{E}$ in the banks of India's most sacred and famous river Ganga close to the Varanasi city, Uttar Pradesh (Fig. 1). The samples were collected from the Trans-Varuna area, which is the floodplain of the Varuna River, a tributary river of Ganga. Since people in the study region depend on the groundwater resources, it is the impetus to understand the groundwater quality. Groundwater is chiefly utilized for residential and farming uses in this area. Development activities such as agriculture, urbanization, and industries often lead to more intensive land use which ultimately causes water pollution (Kibena et al. 2014). This area has a subtropical type climate with a marked monsoon effect.

2.2 Geology and hydrogeology

The Trans-Varuna region is positioned in the northern division of lower Varuna river basin which lies in the middle of the Indo-Gangetic plain cover by the quaternary alluvial

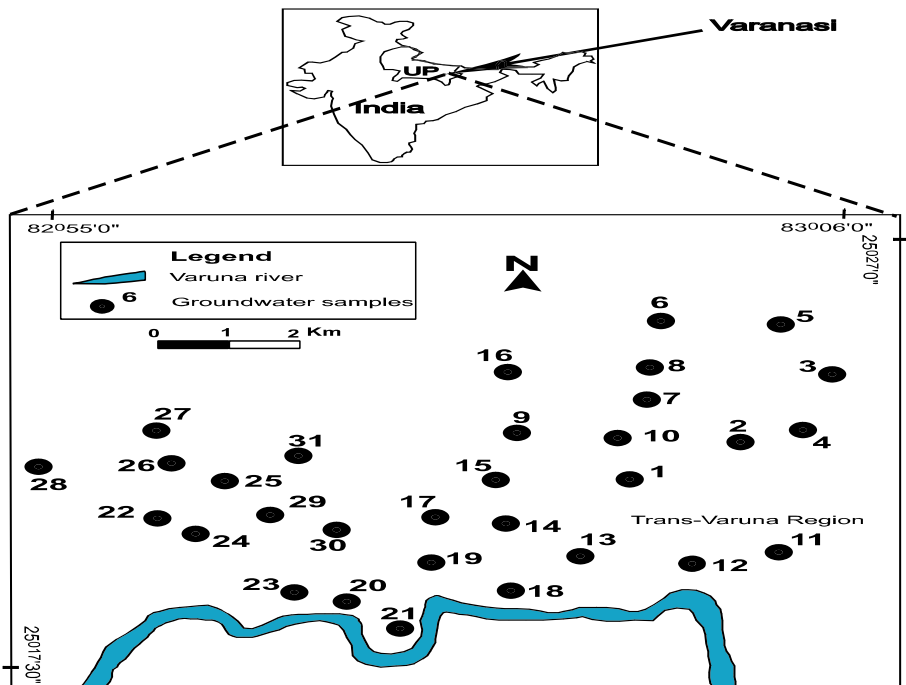


Fig. 1 Location map of Trans-Varuna region, Uttar Pradesh. (1.Ashapur 2. Ledhupur 3. Chiraigaun 4. Rustampur 5. Kitta Umrah 6. Damodarpur 7. Sarnath 8. Mukdarpur 9. Benipur 10. Habelia Chauraha 11. Dinapur 12. Salarpur 13. Sona Talaw 14. Paharia 15. Akatha 16. Parusrampur 17. Pandeypur 18. Nakki Ghat 19. Nai Basti 20. Police Line 21. Chauka Ghat 22. Kadipur Shivpur 23. Company Bagh 24. Kendriya Karagar 25. Shaudhipur 26. Parmanadpur 27. Holapur 28. Tarna 29. UP College 30. Mahaveer Mandir 31. Meerpur Basai)

sediment consist of fine to coarse-grained sand, clay, and clay with kankar. Geologically, alluvial plain of the working area is separated into three discrete sectors, i.e., older alluvial upland, newer alluvial lowland and Holocene to Recent dynamic waterways and floodplains. The presence of yellow–brown sediments with calcareous and ferruginous concentration is the evidence of older alluvial surface. In contrast, the occurrence of the gray-black color organic-rich argillaceous deposits is the indication of Holocene newer alluvial cover. The underlying unconsolidated close to the surface of the majority of the Gangetic plain is usually impending aquifer. Owing to the existence of substitute sand and clay sheets, a multilayer aquifer structure is established in the investigative area. Two distinct sedimentary horizons are found in the study region. One is back swamp clays, containing kankar, at places lying directly below the land surface and having a usual thickness of about 50 m and the other is the underlying average belt deposit, ranging from fine to coarse sand, having an average thickness of 60 m (Shukla and Raju 2008; Shah 2010; Marghade et al. 2011; Raju 2012, Raju et al. 2014).

2.3 Methodology

Groundwater sampling was carried out in May 2013 (premonsoon) and November 2013 (postmonsoon). Thirty-one groundwater samples were taken during premonsoon and again in postmonsoon and from similar sites to assess seasonal variations in groundwater composition. Those hand pumps were preferred for sampling, incessantly useful for drinking and other daily uses. Diverse physiochemical parameters and heavy metals investigations were done as per the practice specified in APHA (2005). pH and EC were deliberated by pH and EC meters, respectively. K and Na were found out by a flame photometer (Elico CL-378). HCO_3 , Ca, Cl and TH were found out by the titrimetric mode and Mg calculated by using TH and Ca. SiO_2 , SO_4 , and NO_3 were computed by UV-3200 double-beam spectrophotometer. F was measured applying Orion ion-selective electrode 4 Star. Heavy metal concentrations of the samples in the post-monsoon season were analyzed by Atomic Absorption Spectrophotometer (M series AAS, Thermo Scientific, Cambridge, UK) using Air-Acetylene Flame. AqQa software package was applied for hydrochemical facies recognition. Statistical parameters like average and correlation were computed by Microsoft Excel Version 2007, and factor investigation was done by using SPSS 16.0. Saturation indices were calculated employing the PHREEQC Interactive 2.12 software. Location map was made by using Surfer 11 while the spatial distribution map of NO_3 was made with the help of Arch GIS 9.3.

3 Results and discussion

3.1 The groundwater chemistry

The statistical outline of chemical ingredient and ionic ration are presented in Table 1.

Among cations, Ca is the principal ion, containing an array of 40 to 102 mg/l and 42 to 112 mg/l, followed by Na ranges from 18.1 to 113.9 mg/l and 24.4 to 135.4 mg/l, than Mg ranges from 15.42 to 54.50 mg/l and 16.58 to 72.49 and K ranges from 1.4 to 8.2 mg/l and 1.9 to 8.1 mg/l in premonsoon and postmonsoon, respectively. Cation chemistry is dominated by Ca, constituting 43% and 41% followed by Na 34% and 33% and Mg 21% and

Table 1 Summary of the different water quality parameters of the groundwater samples

Parameter	WHO limit (1997)	Premonsoon		% Samples exceeding permissible limit WHO (1997)		Postmonsoon		% Samples exceeding permissible limit WHO (1997)	
		Min.	Max.	Mean	Min.	Max.	Mean		
pH	9.2	6.72	7.68	7.25	–	6.94	7.63	7.20	–
EC ($\mu\text{s}/\text{cm}$)		522	1820	915.06	–	494	2260	994.19	–
TDS (mg/l)	1500	276	946	462.68	–	276	1108	503.68	–
Ca (mg/l)	200	40	102	65.61	–	42	112	69.42	–
Mg (mg/l)	150	15.42	54.50	32.06	–	16.58	72.49	40.20	–
Na (mg/l)	200	18.10	113.90	51.64	–	24.40	135.40	56.95	–
K (mg/l)	12	1.40	8.20	3.65	–	1.90	8.10	3.66	–
HCO ₃ (mg/l)	600	212.00	516.00	329.55	–	226.00	644.00	353.48	3
SO ₄ (mg/l)	600	12.80	64.50	34.12	–	16.40	60.42	36.19	–
Cl (mg/l)	600	24.0	128.0	55.4	–	18.00	104.00	59.16	–
F (mg/l)	1.5	0.20	2.50	0.69	3	0.18	1.00	0.66	–
NO ₃ (mg/l)	50	2.40	120.00	36.71	36	12.25	124.50	55.83	52
SiO ₂ (mg/l)	–	28.40	42.26	35.96	–	24.45	40.65	34.37	–
Ca/Mg	–	0.53	3.14	1.44	–	0.49	2.63	1.15	–
Na/Cl	–	0.43	2.97	1.49	–	0.48	3.64	1.62	–
HCO ₃ /(HCO ₃ +SO ₄)	–	0.77	0.95	0.88	–	0.79	0.94	0.88	–

24% of total cations in premonsoon and postmonsoon, respectively and with a minor contribution of K (2%) in both the seasons.

Among the anions, bicarbonate is the principal ion, containing an array of 212 to 516 mg/l and 226 to 644 mg/l followed by chloride ranges from 24 to 128 mg/l and 18 to 104 mg/l than nitrate ranges from 2.4 to 120 mg/l and from 12.25 to 124.4 mg/l, and sulfate ranges from 12.8 to 64.5 mg/l and 16.4 to 64.42 mg/l in premonsoon and postmonsoon, respectively. The anion chemistry of water shows bicarbonate is dominant, constituting 72% and 70% of total anions (TZ⁻) in premonsoon and postmonsoon, respectively followed by chloride 12% and sulfate 7% in both the season.

3.2 Hydrogeochemical facies

Piper graph (Piper 1944) is utilized to classify the water facies depends on the presence of principal ions. From the cationic fields, it is observed that 78% samples in premonsoon and 81% in postmonsoon falls in no dominance type, while 19% and 13% in Ca type and 3% and 6% drops in Mg type in premonsoon and postmonsoon, respectively. While all the samples in postmonsoon and 97% samples in premonsoon fall in bicarbonate type in anionic facies and only 3% samples in premonsoon fall in no dominance type. Investigation of Piper graph suggests that alkaline earth and HCO₃ are the leading ions in the Trans-Varuna region (Fig. 2). The dominance of bicarbonate and calcium ions is the indication of high recharge and cyclic freshening incident working in the alluvial nature of the investigative region (Mizan et al. 2017).

3.3 Sources of ions

3.3.1 Natural processes

Gibbs (1970) projected two charts to recognize the hydrogeological process, which controls the groundwater composition. Gibbs diagram signifies that all the samples of the investigative area are from rock dominance except one sample in postmonsoon season, which is found in evaporation dominance (Fig. 3).

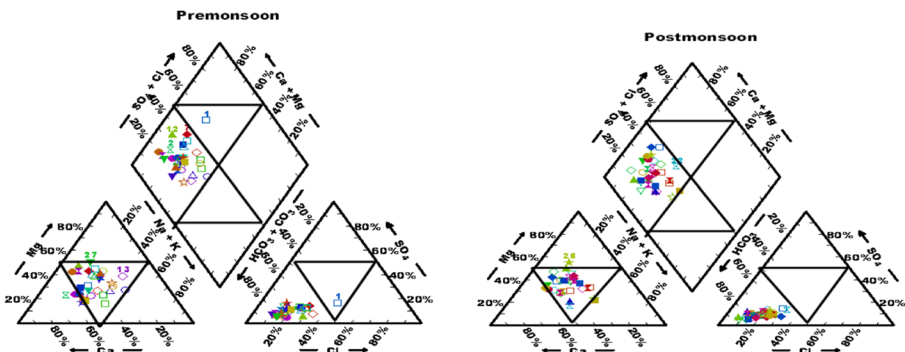


Fig. 2 Relative ionic composition groundwater (after Piper 1944)

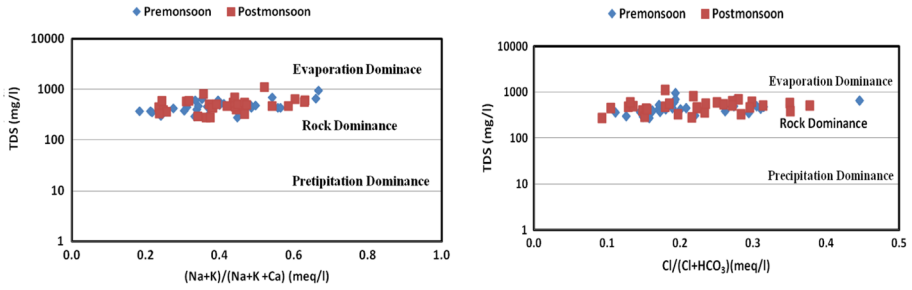


Fig. 3 Mechanism controlling groundwater chemistry (after Gibbs 1970)

The graph between total cations and bicarbonate (Fig. 4a) demonstrates that most of the ion falls above the 1:1 line suggests that carbonate and silicate weathering is contributing ions in the aquifer (Kim et al. 2004). A high relative quotient of $\text{HCO}_3^-/\text{(HCO}_3^- + \text{SO}_4^{2-})$ is the indication of carbonic acid weathering (Pandey et al. 2001; Raju

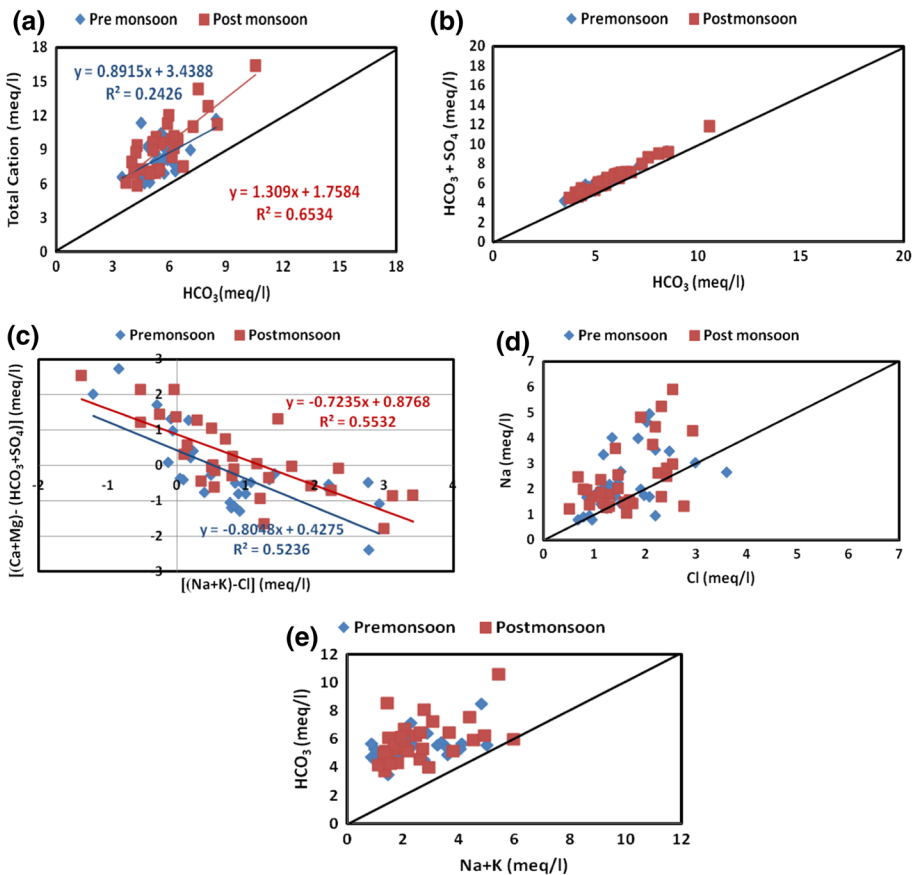


Fig. 4 Relationship between major ionic concentrations

2012). The comparatively elevated quotient of $\text{HCO}_3/(\text{HCO}_3 + \text{SO}_4)$, (> 0.5) in the water samples indicating that carbonic acid is the proton donor during the weathering (Pandey et al. 2001; Raja and Venkatesan 2010). The ratio between HCO_3 and $(\text{HCO}_3 + \text{SO}_4)$ ranges from 0.77 to 0.95 in premonsoon, and 0.79 to 0.94 in postmonsoon points out that carbonic acid is the proton donor in carbonate weathering (Table 1, Fig. 4b). Carbonate weathering procedure in the Trans-Varuna region favoured by the kankar carbonates present in alluvial sediments (Raju et al. 2011).

The cation exchange process is also a significant phenomenon that plays a significant function to determine the groundwater chemistry. A plot amid $[(\text{Na} + \text{K}) - \text{Cl}]$ and $[(\text{Ca} + \text{Mg}) - (\text{HCO}_3 + \text{SO}_4)]$ tells about the possibility of ion exchange process. $[(\text{Na} + \text{K}) - \text{Cl}]$ represent the quantity the (Na + K) achieved/vanished relative to that supplied by the dissolution of chloride salt, while $[(\text{Ca} + \text{Mg}) - (\text{HCO}_3 + \text{SO}_4)]$ represent the quantity of Ca and Mg achieve or loss related to that supplied by dolomite, gypsum and calcite dissolution. If there is no cation exchange process, all the data should plot near to the origin (McLean et al. 2000). If these processes are considered in water chemistry controlling processes, there is a linear relationship between two with a slope of -1 (Jalali 2009). In the study area, the premonsoon data plot shows a slope of -0.804 with an r^2 value of 0.524, and in postmonsoon data plot poses a slope of -0.72 with an r^2 value of 0.553 indicates that ion exchange practice is also a cause of ions in water but in lesser extent (Fig. 4c).

Ca/Mg relation is applied to find out the input of Ca in groundwater. Dolomite dissolution gives an equal quantity of Ca and Mg in water if the Ca/Mg proportion is 1. If Ca/Mg fraction is headed for higher direction indicates that calcite dissolution dominant over the dolomite dissolution in liberating the Ca ion in groundwater. Ca/Mg ratio > 2 is a clear indication of silicate weathering (Kumar et al. 2009). Ca/Mg ratio fluctuates between 0.53 and 3.16 with an average value of 1.44 in premonsoon and 0.49 to 2.63 with an average value of 1.15 in postmonsoon indicates that carbonate weathering is the key reason of Ca in the investigative region (Table 1). A positive and significant correlation between Ca and Cl ($r=0.49$ and $r=0.60$ in premonsoon and postmonsoon, respectively) is the clear indication of the dissolution of chlorapatite mineral (Table 2a, b). In postmonsoon, there is a moderate positive correlation between Ca and Mg ($r=0.41$) suggested that dolomite weathering is the source of both minerals in the study region. While, in premonsoon, there is no positive correlation between these two (Table 2a, b), so at least some amount of Mg in water must be due to the dissolution of aluminosilicate like Biotite $[\text{K}(\text{MgFe})_3(\text{AlSiO}_{10})\text{Fe}(\text{OH})_2]$ and chlorite $[(\text{FeMg})_3(\text{SiAl})_4\text{O}_{10}(\text{OH})_2(\text{FeMg})_3(\text{OH})_6]$ (Marghade et al. 2011).

If the Na/Cl ratio is > 1 it designates that silicate weathering is the basis for Na in water (Meybeck 2003; Jalali 2010). The scattered graph between Na and Cl (Fig. 4d) demonstrates that some of the ions fall on aquiline indicates halite dissolution. In contrast, the majority of the sample falls towards Na side suggests that other sources like silicate weathering and ion exchange process are accountable for the occurrence of Na in groundwater.

Weathering of carbonate minerals and lime kankar found in the alluvial sediments releases bicarbonate in water (Raju 2012). Weathering of silicate minerals like orthoclase, plagioclase, hornblende, olivine, and biotite also released bicarbonate (Kale et al. 2010). The graph of HCO_3 versus Na + K shows a slight inclination toward the bicarbonate (Fig. 4e). The high amount of bicarbonate suggests substantial weathering of rocks, which supports a vigorous mineral dissolution (Stumm and Morgan 1970).

Pyrite (FeS_2) and Gypsum ($\text{CaSO}_4 \cdot 2\text{H}_2\text{O}$) are the two primary source of sulfate in water by rock weathering (Berner and Berner 2012). There is a good to a moderate positive

Table 2 Correlation matrix for the groundwater samples ($N=31$) (a) Premonsoon (b) Postmonsoon

	pH	EC	TDS	Ca	Mg	Na	K	HCO ₃	SO ₄	Cl	F	NO ₃	SiO ₂	TH
(a)														
pH	1													
EC	-0.32	1												
TDS	-0.31	0.99	1											
Ca	-0.47	0.22	0.20	1										
Mg	-0.08	0.33	0.34	-0.26	1									
Na	0.17	0.71	0.71	0.05	0.12	1								
K	-0.32	0.49	0.51	0.38	0.01	0.24	1							
HCO ₃	-0.05	0.45	0.50	-0.04	0.35	0.46	0.42	1						
SO ₄	-0.29	0.54	0.49	0.45	-0.07	0.52	0.18	-0.08	1					
Cl	-0.28	0.54	0.53	0.48	0.34	0.48	0.30	0.04	0.59	1				
F	0.40	-0.12	-0.10	-0.26	-0.02	0.12	-0.18	-0.02	-0.03	-0.20	1			
NO ₃	0.02	0.62	0.56	0.17	0.21	0.55	0.19	-0.04	0.44	0.39	0.08	1		
SiO ₂	0.05	-0.21	-0.20	-0.15	0.13	-0.24	0.06	-0.03	-0.08	-0.24	0.15	-0.17	1	
TH	-0.44	0.46	0.45	0.59	0.63	0.14	0.31	0.26	0.30	0.67	-0.23	0.31	-0.01	1
(b)														
pH	1													
EC	-0.03	1												
TDS	-0.07	0.98	1											
Ca	-0.11	0.56	0.52	1										
Mg	-0.08	0.63	0.57	0.41	1									
Na	0.10	0.59	0.63	0.20	0.15	1								
K	0.07	0.60	0.57	0.51	0.22	0.31	1							
HCO ₃	0.16	0.77	0.70	0.52	0.72	0.48	0.42	1						
SO ₄	-0.32	0.63	0.67	0.62	0.30	0.49	0.48	0.27	1					

Table 2 (continued)

	pH	EC	TDS	Ca	Mg	Na	K	HCO ₃	SO ₄	Cl	F	NO ₃	SiO ₂	TH
Cl	-0.17	0.49	0.51	0.61	0.33	0.53	0.28	0.25	0.65	1				
F	0.10	0.05	0.09	0.03	0.12	0.16	-0.17	0.04	0.05	0.16	1			
NO ₃	-0.07	0.35	0.38	0.27	0.22	0.48	0.29	0.10	0.39	0.44	0.26	1		
SiO ₂	0.39	-0.21	-0.24	-0.17	-0.10	0.02	-0.23	-0.12	-0.10	-0.01	-0.08	-0.19	1	
TH	-0.11	0.71	0.65	0.82	0.86	0.20	0.43	0.75	0.53	0.55	0.09	0.29	-0.16	1

correlation in Ca-SO₄ in premonsoon ($r=0.62$), and postmonsoon ($r=0.45$) suggests the dissolution of gypsum is the source of sulphate in the investigative region.

Various dissolved ions in water are found in a relative proportion to the abundance of their mineral in the surrounding rocks and their solubility (Sarin et al. 1989). Chloroalkane indices are essential to understand the chemical reaction between the rock and water in the duration of residence and movement (Raju 2012). Schoeller (1965) proposed a formula to compute the CAI I and CAI II.

$$\text{CAI I} = [\text{Cl} - (\text{Na} + \text{K})] / \text{Cl}$$

$$\text{CAI II} = [\text{Cl} - (\text{Na} + \text{K})] / (\text{CO}_3 + \text{HCO}_3 + \text{SO}_4 + \text{NO}_3)$$

where all ions are articulated in meq/l.

If CAI values are positive (direct exchange), the exchange process occurs between (Na+K) in water with (Ca+Mg) in rock, and the opposite transfer occurs if the CAI value is negative. In the present study, 20% sample shows positive CAI I and CAI II and 80% samples show negative CAI I and CAI II values in both premonsoon and postmonsoon seasons (Fig. 5).

3.3.2 Anthropogenic input of ions

The high positive correlation of TDS with Na, K, Cl, SO₄, and NO₃ advocates a significant contribution of anthropogenic input of ions in the groundwater. Poor drainage system by the percolation of salty residue in the soil increases the Cl concentration. A modest positive correlation between Ca-Cl ($r=0.48$) and Na-Cl ($r=0.48$) in premonsoon and Ca-Cl ($r=0.61$) and Na-Cl ($r=0.53$) in postmonsoon suggests that halite dissolution and human actions are the key source of Cl in aquifer (Table 2a, b). The high concentration of sulphate suggests the addition of sulphate by the breakdown of organic substance present in soil, fertilizers, and other human influences. Sulphate shows a fine positive correlation with TDS ($r=0.49$) and ($r=0.67$) in premonsoon and postmonsoon, respectively (Table 2a, b) support the anthropogenic influences (Pacheco and Szoc 2006). Na demonstrates a good positive correlation with Cl and SO₄ in both the seasons. It indicates the application of sodium salts (Na₂SO₄) in textile processing unit situated in the study region (Kamal et al. 2016; Madhav et al. 2018b).

The average value of nitrate in premonsoon is within the permitted boundary while in postmonsoon is more than the permissible limit WHO (1997). Spatial distribution of nitrate (Fig. 6) shows a relatively high variation in the southern part of the area along the river in postmonsoon as compare to premonsoon. The elevated concentration of nitrate in

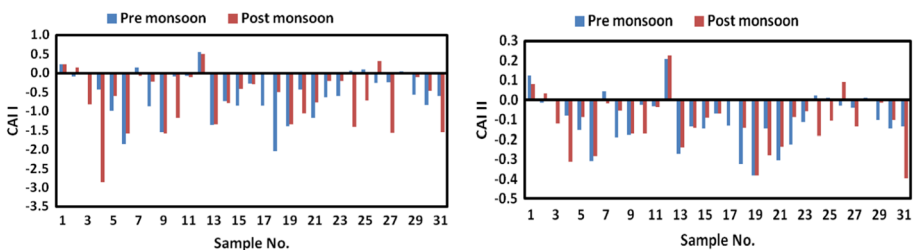


Fig. 5 Chloro alkaline indices plot

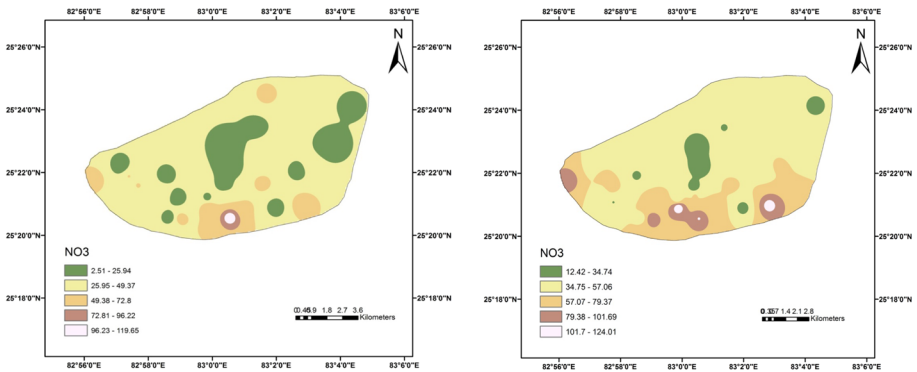


Fig. 6 Spatial distribution of NO_3 in premonsoon and postmonsoon (mg/l)

postmonsoon is maybe owing to deprived management of household sewage and farming runoff, and river water intrusion in nearby aquifers containing high nitrate receiving from the catchment area.

In shallow aquifers, contamination of Nitrate is a common problem owing to mutually point and nonpoint sources (Postma et al. 1991). If the concentration of nitrate in subsurface water is higher than 13, it is considered to be contaminated by human activities and called human affected value (Jalali 2010).

In a saturated aquifer, vertical mixing is relatively slow because high nitrate-containing water flows as plume-like slugs. However, some diffusion between freshwater and nitrate slugs occurs due to the differences in viscosity and specific gravity and laminar flow condition (Handa 1988). Sandy soil is more susceptible to the leakage of nitrate in aquifer than the clayey soil. Clay particles possess negative charges on their surface, which bind with NH_4 and prevent its movement to the aquifer. But clay particles cannot avoid the NO_3 to leaching because NO_3 also contain negative charge which repels by the clay particles. Clay has negligible interpose space for movement, and their pore has lack of oxygen. So facultative anaerobic bacteria use nitrate as an alternative of O_2 and alter it into the N_2 . This procedure is known as denitrification. That's why clayey soil reduces the risk of percolation of NO_3 in groundwater. But sandy soil has considerable pore spaces and high permeability, so sandy soil system aquifer is more vulnerable to NO_3 contamination (Raju et al. 2009). The high values of NO_3 in water are associated with health troubles like methemoglobinemia in newborns and stomach cancer in adult (Walker 1990; Wolfe and Patz 2002; Stadler et al. 2012).

3.3.3 Saturation indices

Saturation index, a mathematical approach is applied to estimate the equilibrium state between groundwater and adjoining rocks (Njitchoua et al. 1997; Almadani et al. 2017). Graphs of SI of calcite indicated that 39% and 41% of samples are undersaturated in terms of calcite in premonsoon and postmonsoon, respectively. While in terms of dolomite, 32% and 29% of samples are undersaturated in premonsoon and postmonsoon, respectively. (Figure 7). The evaluated value of SI of calcite ranged between -0.38 to 0.38 , with an average of 0.057 in premonsoon and ranged between -0.3 to 0.46 with an average of 0.034 in postmonsoon. While the calculated value of dolomite

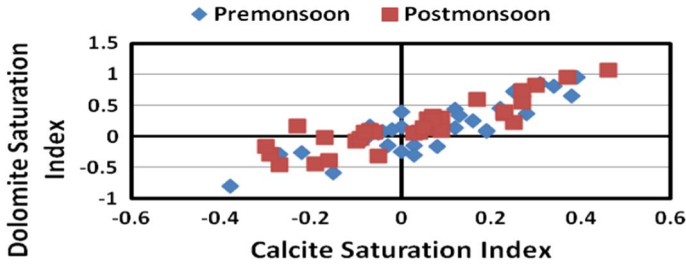


Fig. 7 Relation between saturation indices of calcite and dolomite

is varied between -0.8 to 0.95 , with an average of 0.14 in premonsoon on the other hand in postmonsoon value ranged from -0.046 to 1.07 with an average of 0.18 . A graph between the saturation index of calcite and dolomite indicates that about 60% and 70% of samples are saturated in terms of calcite and dolomite, respectively. There is no significant seasonal variation in the saturation indices of calcite and dolomite (Fig. 7). By the study of the saturation index of the study area, it is understandable that input of the Ca and Mg in the aquifer is owing to the dissolution of saturated and oversaturated carbonate minerals (Raju 2012). Groundwater was saturated regarding chalcedony, goethite, hematite and quartz and undersaturated regarding anhydrite, aragonite, gypsum, halite, and fluorite in both the seasons (Fig. 8).

3.3.4 Statistical screening for water quality data

In the present study, five factors were adequate to explain 80.99% and 81.55% of the variance for the compound matrix in premonsoon and postmonsoon, respectively. (Table 3a, b). The description of various extracted factors is given below:-

3.3.5 Premonsoon

3.3.5.1 Factor 1 (Natural and anthropogenic) It explains the 35.32% of the total variance and shows high positive loading for TDS, SO_4 , Cl, NO_3 and Na. Factor 1 indicates that Na, SO_4 , Cl, and NO_3 ions are responsible for high TDS value. Na has a positive relationship with Cl shows halite weathering (Patel et al. 2016). Cation exchange between Na and Ca

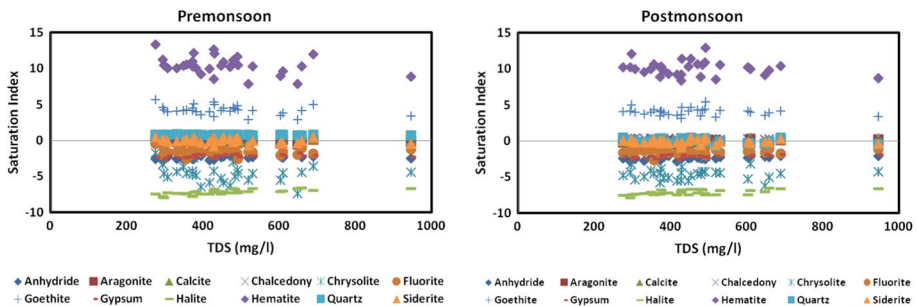


Fig. 8 Plots of saturation indices with respect to different minerals against TDS

Table 3 Varimax rotated component matrix (a) premonsoon (b) postmonsoon

Parameter	Component				
	1	2	3	4	5
<i>(a)</i>					
pH	-.018	-.064	-.797	-.126	.015
EC	.765	.460	.203	.183	-.104
TDS	.726	.519	.193	.184	-.100
Ca	.285	-.087	.802	-.156	.009
Mg	.095	.221	-.092	.952	.070
Na	.795	.425	-.214	-.048	-.154
K	.254	.552	.498	-.155	.245
HCO ₃	.039	.960	-.018	.153	-.028
SO ₄	.778	-.140	.319	-.122	.070
Cl	.640	-.055	.418	.370	-.151
F	.185	-.059	-.592	-.116	.435
NO ₃	.804	-.078	-.068	.160	-.022
SiO ₂	-.206	-.008	-.033	.109	.897
Hardness	.308	.116	.567	.674	.066
Alkalinity	.039	.960	-.018	.153	-.028
Eigen value	5.30	2.25	1.93	1.41	1.06
% Total variance	35.32	16.35	12.87	9.37	7.08
% Cumulative	35.32	51.67	64.53	73.90	80.98
<i>(b)</i>					
pH	-.101	-.037	-.129	.723	-.090
EC	.775	.449	.188	.222	.185
TDS	.709	.459	.268	.247	.207
Ca	.395	.767	-.156	-.190	.118
Mg	.776	.215	.036	-.399	-.009
Na	.396	.308	.625	.428	-.090
K	.366	.497	-.165	.405	.406
HCO ₃	.973	.105	.039	-.004	.031
SO ₄	.195	.840	.164	.092	.073
Cl	.153	.815	.296	.002	-.159
F	.018	-.058	.726	-.309	-.008
NO ₃	.014	.459	.616	-.006	.263
SiO ₂	-.077	-.009	-.080	.117	-.928
Hardness	.711	.565	-.065	-.359	.061
Alkalinity	.973	.105	.039	-.004	.031
Eigen value	6.73	1.79	1.40	1.19	1.09
% Total variance	44.91	11.92	9.32	7.94	7.26
% Cumulative	44.90	56.83	66.15	74.09	81.35

also enrich the Na in water. The positive relation among Na, SO₄, Cl, and NO₃ also suggests the anthropogenic source of these ions in groundwater. The poor municipal waste drainage system and agricultural waste are the key sources of these ions in the aquifer.

3.3.5.2 Factor 2 (Biological Component) It explains 16.35% of the total variance and shows high positive loading for TDS, K, and HCO_3 . The biological decay of organic waste and root respiration generates CO_2 , which produces bicarbonate by reacting H_2O (Raju 2012). K in the water also causes by silicate weathering. Domestic waste and fertilizers used in agriculture are also the sources of K and HCO_3 in groundwater.

3.3.5.3 Factor 3 (Weathering Component) It explains 12.87% of the total variance and shows high positive loading Ca, K and hardness and negative loading of pH and F. High value of hardness is directly associated with Ca. High amounts of Ca in the study region is owing to the carbonate weathering. A relatively low but positive relation of Ca with SO_4 indicates gypsum dissolution is also the sources of Ca in water. The high concentration of Ca ion in a solution prevents the release of F because Ca is negatively associated with F.

3.3.5.4 Factor 4 (Hardness Component) It explains 9.37% of the total variance and shows high loading of Mg and hardness. High values of Mg in water are owing to the carbonate weathering. Hardness is directly associated with Mg salts. MgCl_2 dissolution contributes Mg and Cl in the groundwater. The dissolution of ferromagnesium (amphibole, pyroxene, and biotite minerals) and ion trade amid Ca and Na also contribute Mg in the water.

3.3.5.5 Factor 5 (Geological Component) It describes 7.08% of the total variance and shows high loading of SiO_2 and F. This is a natural factor is due to the geogenic source of SiO_2 and F in groundwater. In premonsoon high temperature accelerate the silica dissolution in water (Khan and Umar 2010).

3.3.6 Postmonsoon

3.3.6.1 Factor 1 (Natural Component) It explains 44.91% of the total variance with a high loading of TDS, Mg, Na, HCO_3 , and hardness. The high value of hardness is directly allied with Ca and Mg. The elevated amount of TDS is owing to the occurrence of Ca, Mg and HCO_3 ions. Ferromagnesium minerals (amphibole, pyroxene, and biotite minerals) and ion exchange between Ca and Na are the possible sources of high concentration of Mg in water. Dissolution of chysorite also provides bicarbonate and Mg to the water. The high value of Ca, Mg and HCO_3 may also be due to the carbonate weathering.

3.3.6.2 Factor 2 (Agriculture Component) It explains 11.92% of the total variance with a high loading of Ca, K, SO_4 , NO_3 , Cl, and hardness. Ca, Cl and SO_4 ions lead to hardness of the water. A good relationship between Ca- SO_4 and K- SO_4 indicates the application of nitrogen fertilizers in agricultural fields. Cation exchange between K and Ca with NH_4 released by nitrogen fertilizer increase the Ca and K concentration in the aquifer. Application of NPK fertilizers in croplands is also contributing K and NO_3 in the groundwater (Schot and Van der Wal 1992).

3.3.6.3 Factor 3 (Geological Component) It explains 9.32% of the total variance with the loading of F, Na, and NO_3 . The high concentration of F is geogenic. Elevated loading of Na and NO_3 is also shown in this factor. High loading of Na is due to the halite weathering while human actions are accountable for the high loading of NO_3 .

3.3.6.4 Factor 4 (Biological Component) It explains 7.94% of the total Variance with the positive loading of pH, Na, and K. The positive loading of pH attributes to the high rate of photosynthesis by autotrophs and, where more CO₂ consumption leads to increase in pH (Omo-Irabor et al. 2008).

3.3.6.5 Factor 5 (Weathering Component) It clarifies 7.26% of the total variance with the positive loading of HCO₃ and negative loading of SiO₂. The high value of bicarbonate in the Trans–Varuna region is owing to the carbonate weathering favoured by the kankar carbonates. The dissolved bicarbonate in groundwater is also produced by the reaction of rainwater and CO₂, originated from root respiration and humus decay (Raju et al. 2009).

3.3.7 Groundwater for drinking

According to Davis and De Wiest (1966) cataloguing, all samples in premonsoon and 97% samples in postmonsoon are permissible for human consumption (Table 4). Based on the Freez and Cherry (1979) cataloguing, all the samples in premonsoon and 97% samples in postmonsoon belong to a freshwater category and 3% sample in postmonsoon fall in brackish water type. Based on the Sawyer and Mc Carty (1967) cataloguing 68% and 42% of samples are moderately hard, and 32% and 58% of samples are very hard in premonsoon and postmonsoon, respectively. Excessive alkalinity in water may cause eye irritation and harmful to soil and plants. Overall most of the parameter is inside the permissible limit (WHO 1997) in both seasons. Still, the values of NO₃ in 36% and 52% of samples are above the allowable limit approved by WHO (1997) in premonsoon and postmonsoon, respectively.

3.3.8 Groundwater for irrigation

The quantity and chemistry of dissolved ions in water set up its quality for farming purpose. An unnecessary amount of dissolved constituents in irrigation water modify soil configuration, permeability, and exposure to air that openly influence crop development (Rao et al. 2002; Alam et al. 2012). Na concentration is a significant factor in the evolution of water quality for cultivation use because Na decreases the permeability of water (Jeevanandam et al. 2012). Increase salinity due to Long-term irrigation is harmful to soil and plant as high salinity lowers the crop yield and eliminates the native vegetation (Misra and Mishra 2007). Various parameters are used to recognize the condition of groundwater for agriculture consumption.

3.3.9 Residual sodium carbonate

RSC is applied to find out the damaging outcomes of HCO₃ on water quality for farming use (Eaton 1950). The subsequent formula can calculate RSC:

$$\text{RSC} = (\text{CO}_3 + \text{HCO}_3) - (\text{Ca} + \text{Mg})$$

where ionic values are articulated in meq/l.

Irrigation water having an elevated value of RSC directs to amplification in the adsorption of Na on soil (Eaton 1950). Water containing RSC over 2.5 meq/l is not apt for

Table 4 Categorization of groundwater for different purpose

Quality parameter	Range	Classification	(% of samples)	
			Premonsoon	Postmonsoon
TDS (Davis and De Wiest 1966)	< 500	Desirable for drinking	74	55
	500–1000	Permissible for drinking	26	42
	1000–3000	Useful for agriculture	–	3
	> 3000	Unfit for drinking and irrigation	–	–
TDS (Freeze and Cherry 1979)	< 1000	Fresh Water	100	97
	1000–10,000	Brackish Water	–	3
	10,000–100,000	Saline water	–	–
	> 1,000,000	Brine water	–	–
Hardness (Sawyer and Mc Carty 1967)	< 75	Soft	–	–
	75–150	Slightly hard	–	–
	150–300	Moderately hard	68	42
	> 300	Very hard	32	58
	0–20	Excellent	19	26
	20–40	Good	68	65
	40–60	Permissible	13	9
Na % (meq/l)	60–80	Doubtful	–	–
	> 80	Unsuitable	–	–
	0–10	Excellent	100	100
	10–18	Good	–	–
	18–26	Fair	–	–
SAR (meq/l)	> 26	Poor	–	–
	< 1.25	Good	97	97
	1.25–2.5	Medium	3	3
	> 2.5	Bad	–	–

Table 4 (continued)

Quality parameter	Range	Classification	(% of samples)	
			Premonsoon	Postmonsoon
EC ($\mu\text{S}/\text{cm}$)	<250	Low salinity hazards	–	–
	250–750	Medium salinity hazard	29	19
	750–2250	C3 high salinity hazard	71	78
	>2250	Very high salinity hazard	–	3

agricultural use while water containing RSC more than 5 mg/l is not fit for the growth of plants (Singh et al. 2011). On the bases of RSC, water can be sorted in 3 groups such as safe, marginally suitable and unsuitable. In the current investigation, it is established that 97% of samples in both the seasons lie in the safe category, and only 3% sample lies in the marginally suitable group (Table 4).

3.3.10 Electrical conductivity and percentage of sodium

EC and Na play a critical role to conclude the condition of water for farming use. Based on EC values, Richard (1954) sorted the irrigational water in four sets such as low, medium, high, very high. The subsequent formula can calculate % Na:

$$\%Na = (Na + K)/(Ca + Mg + Na) \times 100$$

The values of % Na ranged from 10.65 to 47.98 in premonsoon and between 12.88 to 49.49 in postmonsoon. When sorted based on % Na only 19% samples are excellent, 68% is good, and 13% is permissible in premonsoon, and 26% samples are excellent, 65% is good, and 9% is permissible in a postmonsoon season (Table 4).

Wilcox (1948) sorted groundwater for irrigation, (depends on % Na and EC) in five different scales of fitness. Wilcox diagram (Fig. 9) relevant that 26% samples fall under excellent to good, and 74% samples lies in good to permissible range in premonsoon. In comparison, in

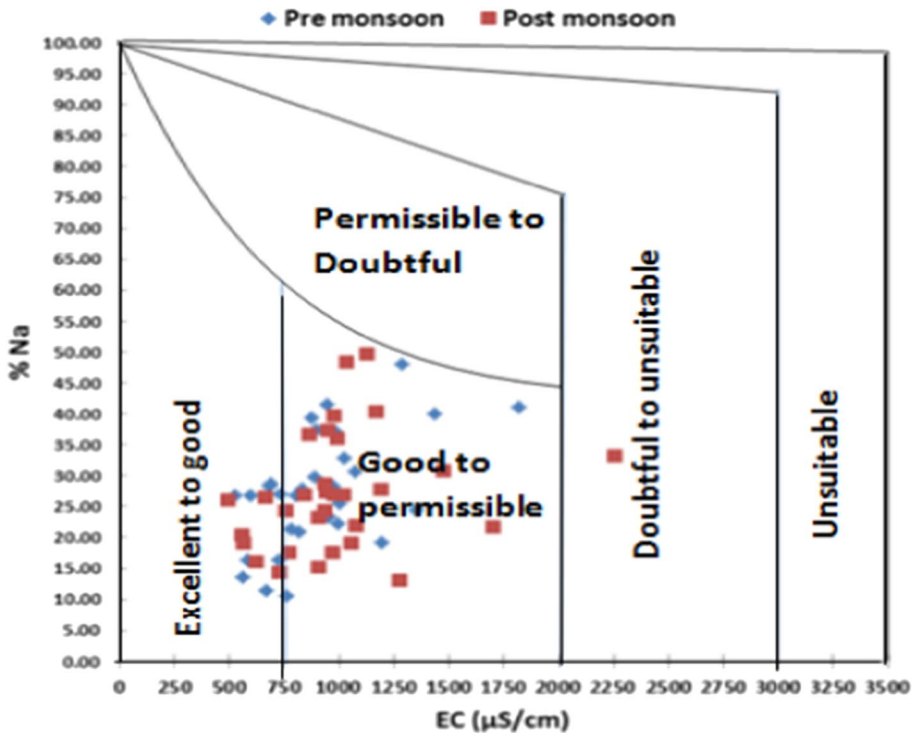


Fig. 9 Categorization of groundwater on the basis of electric conductivity and % sodium (after Wilcox 1948)

postmonsoon 19% samples fall under excellent to good, 77% samples lies in good to permissible range 3% samples is found in doubtful to the unsuitable area.

3.3.11 U S salinity diagram (1954)

The sodium hazard is articulated in the term of SAR. The SAR value is determined by applying Richard (Richards 1954) equation:

$$SAR = Na / \sqrt{(Ca + Mg) / 2}$$

where ionic values are articulated in meq/l.

Based on Sodium adsorption ratio, agricultural water can be characterized into four groups as Excellent, good, fair and poor. All the samples of the studied region lie into the excellent class in both the seasons (Table 4).

More comprehensive irrigation appropriateness analysis can be achieved by plotting a USSL graph. The USSL graph is applied extensively for categorized irrigation water where SAR schemes against EC (Richards 1954). The USSL graph reveals that most of the samples drop in the class of C2S1 and C3S1 category. C2S1 and C3S1 type of water can be utilized for agriculture purpose on approximately all types of soil having a small threat to transferable Na. However, one sample in postmonsoon season falls in C4S1 category (Fig. 10). This type of water can use for high salt-tolerant plants (Karnath 1987; Raju et al. 2009).

3.3.12 Evaluation of noncarcinogenic hazard intensity of NO₃

In this study, the health hazard from non-carcinogenic disclosure encouraged by the NO₃ in water by the ingestion route was done for human in different age groups. The Chronic daily intake (CDI) values can be estimated by the subsequent formula (Miri et al. 2018):

$$CDI = (C_w \times DI \times EF \times EP) / (BW \times AT)$$

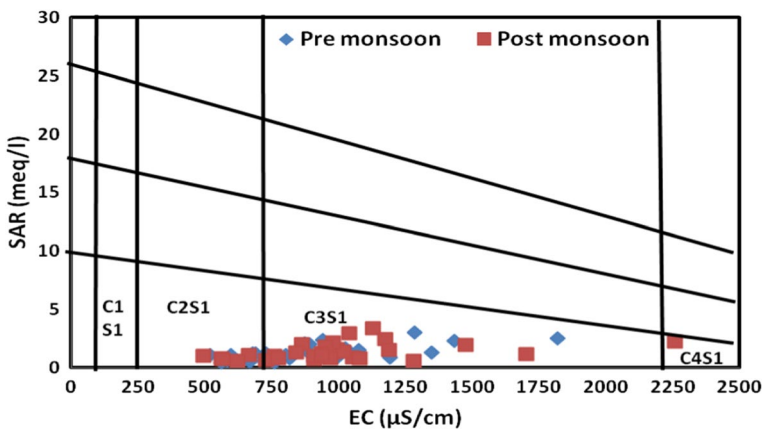


Fig. 10 Categorization of groundwater in relation to salinity hazard and sodium hazard (after USSL Diagram 1954)

where C_w is the value of NO_3 in water, DI is everyday water ingestion (L/Day), EF is exposure regularity (days/year), EP is the average exposure time (years), BW is average body weight (kg) and AT is the average time (days). Here DI is 2, 1.5 and 0.8 L for adult, children, and infants respectively. EP is 40, 10 and 1 year and BW values are 70, 40 and 10 kg for an adult, children, and infants respectively (Qasemi et al. 2018). CDI values for three diverse age fractions are specified in Table 5.

Hazard quotient (HQ) is a fraction of the possible exposure to a pollutant and stage at which no destructive outcomes are likely. The HQ value is calculated by the subsequent formula (Radfard et al. 2018):

Table 5 Chronic daily intake (mg/kg/day) values for 3 different age groups

Sample no.	Premonsoon			Postmonsoon		
	CDI (Adult)	CDI (Children)	CDI (Infant)	CDI (Adult)	CDI (Children)	CDI (Infant)
1	1.78	2.33	4.98	1.87	2.45	5.24
2	0.29	0.38	0.81	1.34	1.76	3.75
3	0.17	0.22	0.48	1.44	1.89	4.02
4	1.41	1.85	3.94	1.76	2.3	4.92
5	0.66	0.87	1.86	0.9	1.18	2.51
6	1.62	2.12	4.53	1.45	1.9	4.06
7	1.37	1.8	3.85	1.29	1.69	3.6
8	0.4	0.52	1.11	0.97	1.27	2.7
9	0.07	0.09	0.19	0.35	0.46	0.98
10	1.2	1.58	3.36	1.31	1.72	3.68
11	2.04	2.68	5.71	3.22	4.22	9.01
12	0.24	0.32	0.67	0.7	0.92	1.97
13	1.53	2	4.27	2.04	2.67	5.71
14	1.3	1.71	3.65	1.68	2.2	4.7
15	0.15	0.2	0.43	0.53	0.7	1.49
16	0.22	0.29	0.62	0.58	0.77	1.64
17	0.5	0.65	1.39	1.08	1.42	3.03
18	3.43	4.5	9.6	2.94	3.86	8.23
19	2.07	2.72	5.79	3.56	4.67	9.96
20	1.77	2.33	4.96	2.82	3.7	7.89
21	1.49	1.95	4.16	2.11	2.77	5.9
22	0.77	1.01	2.16	1.09	1.43	3.06
23	0.38	0.5	1.06	1.33	1.74	3.72
24	0.91	1.2	2.56	0.97	1.28	2.73
25	1.47	1.93	4.12	2.07	2.72	5.8
26	1.44	1.89	4.02	1.81	2.38	5.07
27	0.19	0.25	0.54	1.21	1.59	3.4
28	1.87	2.46	5.24	2.83	3.72	7.93
29	0.35	0.47	0.99	1.78	2.34	4.98
30	0.92	1.21	2.58	1.59	2.09	4.45
31	0.5	0.66	1.4	0.84	1.1	2.34

$$HQ = CDI/RfD$$

where RfD is the mentioned dose of NO_3 i.e. 1.6 mg/kg/day.

If the HQ value is more than one it causes negative health consequences on the exposed person. The finding shows that HQ values of NO_3 range from 0.04 to 2.14 and 0.22 to 2.22 for adults, 0.06 to 2.81 and 0.29 to 2.92 for children and 0.12 to 6.00 and 0.61 to 6.23 for an infant in premonsoon and postmonsoon respectively. The HQ values for 22% and 41% adult in premonsoon and postmonsoon, respectively were more than 1, HQ values for 45% and 64% children in premonsoon and postmonsoon, respectively were more than one and HQ values for 67% and 93% infants were more than 1 suggesting the groundwater has severe health impacts on those exposed individuals of respective age groups. Thus infants and children are more susceptible to nitrate contamination as compared to adults.

3.3.13 Heavy metals

The source of trace metals in an aquifer is through the natural phenomenon like weathering of rock mineral and anthropogenic activities like agricultural activities, release of sewage, traffic emission and waste discarding (CPCB 2008). Table 6 shows the heavy metal concentration in the groundwater samples in Trans-Varun region. The samples show values more than the permissible limit laid by WHO (1997) are highlighted in Table 6. Fe shows high variance and 74% samples are beyond the allowable limit of WHO (1997). Heavy contamination of Fe may be owing to the dissolution of iron-rich minerals (pyrites, limonite, and goethite) and municipal sewage effluent leaching in the aquifer (Raju et al. 2011). Pb is beyond the permissible limit in 9% samples. Heavy traffic emits lead into the atmosphere, and it creates water pollution. 19% of samples are beyond the allowable limit of Ni. A higher value of Ni in some samples may be due to effluents of textile dye houses presented in the study region.

3.3.14 Target hazard quotient and probable health hazard

Heavy metals go into the human body by several pathways, but in contrast to oral ingestion, inhalation and dermal absorption are considered as irrelevant (Khan et al. 2013). The health hazard originated by heavy metal contact is classically demonstrated by the THQ (USEPA 1986). THQ is in general non-cancer hazard evaluation mode founded on a ratio between the approximate dosage of pollutant and the reference dosage underneath which there will not be any significant hazard (Pawar and Pawar 2016 and Ahamad et al. 2018). The non-carcinogenic noxious risk is measured to be less if the THQ and HI value is < 1. Once it departs ahead of 1, a probable health hazard might take place.

$$THQ = (EFr \times ED_{tot} \times SFI \times MCS_{inorg}) / (RfD \times BWa \times ATn)$$

where EFr is exposure regularity (365 days/year); ED is contact interval (70 years, equal to normal lifetime); SFI is water intake rate (5L/person/day); MCS_{inorg} is the metal quantity in sample ($\mu\text{g/L}$); BWa is standard body weight (55.9 kg for adult); ATn is time interval over when dose is averaged (365 days/year \times ED_{tot}), and RfD is oral reference dose ($\mu\text{g/kg/day}$). RfD values for Fe, Mn, Cu, Zn, Pb, Cd, Ni, and Cr are 300, 20, 300, 40, 0.4, 0.5, 20 and 3, in that order (US EPA 2000; Ahamad et al. 2018). The collective non-carcinogenic outcome for many heavy metals can be illustrated by Hazard Index (HI):

Table 6 Heavy metals concentrations ($\mu\text{g/L}$) in groundwater samples

Sample	Fe	Mn	Cu	Zn	Co	Pb	Ni
1	702.9	45.1	104.7	312.1	33.8	6.28	BDL
2	325.4	2.8	50.3	211.4	48.9	1.8	BDL
3	365.4	50.1	118.4	453.1	42.2	7.98	BDL
4	428.2	2.1	118.0	41.9	71.6	BDL	BDL
5	522.1	32.5	4.6	98.3	62.3	4.29	10.23
6	394.6	9.87	16.8	245.0	51.7	2.27	BDL
7	433.4	6.5	32.2	298.0	56.3	8.75	10.63
8	141.6	49.8	6.4	189.7	51.6	9.9	BDL
9	565.2	3.1	47.9	265.7	74.4	8.87	BDL
10	487.8	56.3	2.2	248.0	49.3	5.89	42.4
11	315.8	23.4	9.8	312.5	39.8	4.63	13.2
12	308.3	19.8	34.6	274.0	71.1	6.03	BDL
13	130.9	13.7	45.2	123	49.9	8.52	BDL
14	58.7	73.9	98.6	89.6	68.4	2.49	67.5
15	284.6	18.6	30.4	302.4	60.5	3.71	17.1
16	346.1	24.6	89.0	66.7	50.8	11.67	19.6
17	289.7	50.3	120.5	123.3	54.8	4.89	26.8
18	875.7	47.8	53.2	9.3	62.3	BDL	39.3
19	322.4	37.8	37.9	79.9	49.8	5.12	24.2
20	136.6	46.5	10.5	142.0	68.7	2.34	10.98
21	454.6	26.4	65.5	392.9	60.6	6.38	14.5
22	168.4	164.2	106.9	263.6	57.5	6.84	BDL
23	412.7	42.1	83.6	300.1	59.2	10.74	10.8
24	500.1	337.9	5.3	318.6	60.6	4.37	16.2
25	399.8	64.2	7.6	258.1	43.5	6.44	BDL
26	466.7	37.3	27.8	193.9	31.6	3.28	BDL
27	407.9	22.3	46.3	200.1	36.5	13.94	BDL
28	1262.3	11.9	138	69.5	48.9	9.02	16.7
29	98.4	21.2	62.3	162.4	67.2	4.94	BDL
30	835.3	15.5	34.9	139.7	55.1	5.10	24.2
31	1376.5	84.7	115.4	118.6	53.4	3.67	BDL

$$\text{HI} = \sum_{i=1}^n \text{HQ}$$

The values of THQ of the considered metals in TransVaruna regions are summarized in Table 7. THQ value was established in the sequence of $\text{Pb} > \text{Zn} > \text{Mn} > \text{Fe} > \text{Ni} > \text{Cu}$. The THQ of metals varies from Fe (0.018–0.410 with a average of 0.133), Mn (0.009–1.511 with a average of 0.208), Cu (0.001–0.041 with a average of 0.017), Zn (0.000–1.013 with a average of 0.443), Pb (0.000–3.117 with a average of 1.33), Ni (0.000–0.302 with a average of 0.053). It is viewed that Fe, Mn, Cu, Zn, and Ni metals show THQ values < 1 , whereas Pb (64.5% samples) presetting > 1 THQ values. The water samples with high THQ value (> 1) for Pd, Zn, and Mn will have probable human health hazard if these groundwaters are being utilized for the extended period without

Table 7 Target Hazard Quotient (THQ) and potential human health risk (HI) in groundwater samples

Sample no.	Fe	THQ	Mn	THQ	Cu	THQ	Zn	THQ	Pb	THQ	Ni	THQ	HI
1	702.9	0.210	45.1	0.202	104.7	0.031	312.1	0.698	6.28	1.404	0	0.000	2.545
2	325.4	0.097	2.8	0.013	50.3	0.015	211.4	0.473	1.8	0.403	0	0.000	1.000
3	365.4	0.109	50.1	0.224	118.4	0.035	453.1	1.013	7.98	1.784	0	0.000	3.166
4	428.2	0.128	2.1	0.009	118	0.035	41.9	0.094	0	0.000	0	0.000	0.266
5	522.1	0.156	32.5	0.145	4.6	0.001	98.3	0.220	4.291	0.960	10.23	0.046	1.527
6	394.6	0.118	9.87	0.044	16.8	0.005	245	0.548	2.27	0.508	0	0.000	1.222
7	433.4	0.129	6.5	0.029	32.2	0.010	298	0.666	8.75	1.957	10.63	0.048	2.838
8	141.6	0.042	49.8	0.223	6.4	0.002	189.7	0.424	9.9	2.214	0	0.000	2.905
9	565	0.168	3.1	0.014	47.9	0.014	265.7	0.594	8.87	1.983	0	0.000	2.774
10	487.8	0.145	56	0.250	2.2	0.001	248	0.555	5.89	1.317	42.4	0.190	2.458
11	315.8	0.094	23.4	0.105	9.8	0.003	312.5	0.699	4.628	1.035	13.2	0.059	1.994
12	308.3	0.092	19.8	0.089	34.6	0.010	274	0.613	6.032	1.349	0	0.000	2.152
13	130.9	0.039	13.7	0.061	45.2	0.013	123	0.275	8.52	1.905	0	0.000	2.294
14	58.7	0.018	73.9	0.331	98.6	0.029	0	0.000	2.49	0.557	67.5	0.302	1.236
15	284.6	0.085	18.6	0.083	30.4	0.009	302.4	0.676	3.71	0.830	17.1	0.076	1.759
16	346.1	0.103	24	0.107	89	0.027	0	0.000	11.67	2.610	19.6	0.088	2.934
17	289.7	0.086	50	0.224	120.5	0.036	123	0.275	4.89	1.093	26.8	0.120	1.834
18	875	0.261	47	0.210	53.2	0.016	9.3	0.021	0	0.000	39.3	0.176	0.683
19	322.4	0.096	37.8	0.169	37.9	0.011	79.9	0.179	5.123	1.146	24.2	0.108	1.709
20	136.6	0.041	46.5	0.208	10.5	0.003	142	0.318	2.34	0.523	10.98	0.049	1.142
21	454.6	0.136	26.4	0.118	65.5	0.020	392.9	0.879	6.38	1.427	14.5	0.065	2.643
22	168.4	0.050	164.2	0.734	106.9	0.032	263	0.588	6.84	1.530	0	0.000	2.934
23	412.7	0.123	42.1	0.188	83.6	0.025	300.1	0.671	10.74	2.402	10.8	0.048	3.457
24	500.1	0.149	337.9	1.511	5.3	0.002	318.6	0.712	4.372	0.978	16.2	0.072	3.424
25	399.8	0.119	64.2	0.287	7.6	0.002	258.1	0.577	6.442	1.441	0	0.000	2.426

Table 7 (continued)

Sample no.	Fe	THQ	Mn	THQ	Cu	THQ	Zn	THQ	Pb	THQ	Ni	THQ	HI
26	466.7	0.139	37	0.165	27.8	0.008	193.9	0.434	3.281	0.734	0	0.000	1.480
27	407.9	0.122	22.3	0.100	46.3	0.014	200.1	0.447	13.94	3.117	0	0.000	3.800
28	1262.3	0.376	11.9	0.053	138	0.041	69	0.154	9.02	2.017	16.7	0.075	2.717
29	98	0.029	21.2	0.095	62.3	0.019	162	0.362	4.94	1.105	0	0.000	1.610
30	835.3	0.249	15.5	0.069	34.9	0.010	139.7	0.312	5.102	1.141	24.2	0.108	1.890
31	1376.5	0.410	84.7	0.379	115.4	0.034	118.6	0.265	3.671	0.821	0	0.000	1.910

the appropriate remedial course. The HI value of metals fluctuates from 0.266 to 3.88 with an average of 2.13. 93.5% of samples in the study area show HI greater than one value.

4 Conclusion

Various geochemical ionic relation verifies that predominant hydrogeochemical processes are accountable for the chemical composition of the groundwater. The result exposed that carbonate mineral weathering and human actions are the leading factors governing the primary ion composition in the study region. After the interpretation of various physicochemical parameters, it is viewed that the bulk of samples in both seasons descends in the section of alkaline earth and weak acidic conditions (Ca–Mg–HCO₃ type). According to the Gibbs plot, the hydrogeochemistry of samples points out that all the samples are from rock dominance, except one sample in post moon that shows evaporation dominance. 80% of the samples show the negative value of Chloroalkaline indices which indicates the indirect exchange of ions in the study region. Principle component analysis advocates that geogenic, weathering, agricultural activities and biological decay are key processes accountable for hydrogeochemical features of groundwater in Trans-Varuna region. In terms SAR, % Na, RSC, Wilcox diagram and USSL graph of the majority of the groundwater is fit for irrigation in both the seasons. 36% samples in premonsoon and 52% samples in postmonsoon are containing NO₃ concentration beyond the permissible limit (> 45 mg/l) which requirements corrective methods before drinking use. NO₃ in the groundwater is mainly owing to the human-induced like agricultural runoff and domestic sewage waste. Human exposure to NO₃ through ingestion was in the subsequent direct Infant > Children > Adult. High Fe values in the majority of water samples may be due to iron-rich minerals and anthropogenic actions. The water samples with high THQ value (> 1) for Pd, Zn, and Mn will have probable human health hazard if these groundwaters are being utilized for the extended period devoid of appropriate corrective methods.

Acknowledgements The first author (SM) is thankful to the University Grants Commission (UGC) for financial assistance under the UGC NET-JRF Fellowship program (2012-'17). NJR is profoundly grateful UGC for financial support under SAP-DSA II program and 21st century Indo-US Research initiative 2014 of JNU and MSU (clean energy& water research) and also for DST for purse grant and UPOE (ID-170) funds under "Holistic Development program". SM is grateful to Mr. Umakant and Mr. Ganesh Datt Mishra for their help during the field work and sampling campaign.

References

- Ahamad, A., Raju, N. J., Madhav, S., Gossel, W., & Wycisk, P. (2018). Impact of non-engineered Bhalswa landfill on groundwater from Quaternary alluvium in Yamuna flood plain and potential human health risk, New Delhi, India. *Quaternary International*.
- Alam, M., Rais, S., & Aslam, M. (2012). Hydrochemical investigation and quality assessment of ground water in rural areas of Delhi, India. *Environmental Earth Sciences*, 66(1), 97–110.
- Almadani, S., Alfaihi, H., Al-Amri, A., Fnais, M., Ibrahim, E., Abdelrahman, K., et al. (2017). Hydrochemical characteristics and evaluation of the granite aquifer in the Alwadeen area, southwest Saudi Arabia. *Arabian Journal of Geosciences*, 10(6), 139.
- APHA. (2005). *Standard method for examination of water and wastewater* (21st ed.). Washington: American Public Health Association.
- Arnade, L. J. (1999). Seasonal correlation of well contamination and septic tank distance. *Groundwater*, 37(6), 920–923.

- Berner, E. K., & Berner, R. A. (2012). *Global environment: Water, air, and geochemical cycles*. Princeton: Princeton University Press.
- Central Pollution Control Board (2008) Status of Groundwater Quality in India – Part – II.
- Chandran, S., Karmegam, M., Kumar, V., & Dhanasekarapandian, M. (2017). Evaluation of groundwater quality in an untreated wastewater irrigated region and mapping: A case study of Avaniyapuram sewage farm, Madurai. *Arabian Journal of Geosciences*, *10*(7), 159.
- Chkirbene, A., Tsujimura, M., Charef, A., & Tanaka, T. (2009). Hydro-geochemical evolution of groundwater in an alluvial aquifer: Case of Kurokawa aquifer, Tochigi prefecture, Japan. *Desalination*, *246*(1–3), 485–495.
- Davis, S. N., & DeWiest, R. J. (1966). *Hydrogeology* (No. 551.49 D3).
- Eaton, F. M. (1950). Significance of carbonates in irrigation waters. *Soil Science*, *69*(2), 123–134.
- Elangovan, N. S., Lavanya, V., & Arunthathi, S. (2017). *Assessment of groundwater contamination in a sub-urban area of Chennai, Tamil Nadu, India* (pp. 1–13). Development and Sustainability: Environment.
- Freeze, R. A., & Cherry, J. A. (1979). *Groundwater* (p. 604). Englewood Cliffs, NJ: Prentice-Hall.
- Gibbs, R. J. (1970). Mechanisms controlling world water chemistry. *Science*, *170*(3962), 1088–1090.
- Hamzah, Z., Aris, A. Z., Ramli, M. F., Juahir, H., & Narany, T. S. (2017). Groundwater quality assessment using integrated geochemical methods, multivariate statistical analysis, and geostatistical technique in shallow coastal aquifer of Terengganu, Malaysia. *Arabian Journal of Geosciences*, *10*(2), 49.
- Hancock, P. J., Boulton, A. J., & Humphreys, W. F. (2005). Aquifers and hyporheic zones: Towards an ecological understanding of groundwater. *Hydrogeology Journal*, *13*(1), 98–111.
- Handa, B. K. (1988). Content of potassium in groundwater in India. *Fertilizer News*, *33*(11), 15–27.
- Hem, J. D. (1991). *Study and interpretation of the chemical characteristics of natural water*, 2254 (3rd ed., p. 263). Jodhpur: Scientific Publication.
- Huang, G., Sun, J., Zhang, Y., Chen, Z., & Liu, F. (2013). Impact of anthropogenic and natural processes on the evolution of groundwater chemistry in a rapidly urbanized coastal area, South China. *Science of the Total Environment*, *463*, 209–221.
- Jalali, M. (2009). Geochemistry characterization of groundwater in an agricultural area of Razan, Hamadan, Iran. *Environmental Geology*, *56*(7), 1479–1488.
- Jalali, M. (2010). Groundwater geochemistry in the Alisadr, Hamadan, western Iran. *Environmental Monitoring and Assessment*, *166*(1–4), 359–369.
- Jeevanandam, M., Nagarajan, R., Manikandan, M., Senthilkumar, M., Srinivasalu, S., & Prasanna, M. V. (2012). Hydrogeochemistry and microbial contamination of groundwater from lower ponnaiyar basin, cuddalore district, Tamil Nadu, India. *Environmental Earth Sciences*, *67*(3), 867–887.
- Kale, S. S., Kadam, A. K., Kumar, S., & Pawar, N. J. (2010). Evaluating pollution potential of leachate from landfill site, from the Pune metropolitan city and its impact on shallow basaltic aquifers. *Environmental Monitoring and Assessment*, *162*(1–4), 327–346.
- Kamal, A. K. I., Ahmed, F., Hassan, M., Uddin, M., & Hossain, S. M. (2016). Characterization of textile effluents from dhaka export processing zone (DEPZ) Area in Dhaka, Bangladesh. *Pollution*, *2*(2), 153–161.
- Karanth, K. R. (1987). *Groundwater assessment development and management* (p. 725). New Delhi: Tata McGraw Hill Publishing Company Ltd.
- Kenoyer, G. J., & Bowser, C. J. (1992). Groundwater chemical evolution in a sandy silicate aquifer in northern Wisconsin: 1. Patterns and rates of change. *Water Resources Research*, *28*(2), 579–589.
- Khan, K., Lu, Y., Khan, H., Zakir, S., Khan, S., Khan, A. A., et al. (2013). Health risks associated with heavy metals in the drinking water of Swat, northern Pakistan. *Journal of Environmental Sciences*, *25*(10), 2003–2013.
- Khan, M. M. A., & Umar, R. (2010). Significance of silica analysis in groundwater in parts of Central Ganga Plain, Uttar Pradesh, India. *Current Science*, *98*(9), 1237–1240.
- Kibena, J., Nhapi, I., & Gumindoga, W. (2014). Assessing the relationship between water quality parameters and changes in landuse patterns in the Upper Manyame River, Zimbabwe. *Physics and Chemistry of the Earth, Parts A/B/C*, *67*, 153–163.
- Kim, K., Rajmohan, N., Kim, H. J., Hwang, G. S., & Cho, M. J. (2004). Assessment of groundwater chemistry in a coastal region (Kunsan, Korea) having complex contaminant sources: A stoichiometric approach. *Environmental Geology*, *46*(6–7), 763–774.
- Kumar, M., Kumari, K., Singh, U. K., & Ramanathan, A. L. (2009). Hydrogeochemical processes in the groundwater environment of Muktsar, Punjab: Conventional graphical and multivariate statistical approach. *Environmental Geology*, *57*(4), 873–884.
- Lu, K. L., Liu, C. W., Wang, S. W., Jang, C. S., Lin, K. H., Liao, V. H. C., et al. (2011). Assessing the characteristics of groundwater quality of arsenic contaminated aquifers in the blackfoot disease endemic area. *Journal of Hazardous Materials*, *185*(2–3), 1458–1466.

- Madhav, S., Ahamad, A., Kumar, A., Kushawaha, J., Singh, P., & Mishra, P. K. (2018a). Geochemical assessment of groundwater quality for its suitability for drinking and irrigation purpose in rural areas of Sant Ravidas Nagar (Bhadohi), Uttar Pradesh. *Geology, Ecology, and Landscapes*, 2(2), 127–136.
- Madhav, S., Ahamad, A., Singh, P., & Mishra, P. K. (2018b). A review of textile industry: Wet processing, environmental impacts, and effluent treatment methods. *Environmental Quality Management*, 27(3), 31–41.
- Marghade, D., Malpe, D. B., & Zade, A. B. (2011). Geochemical characterization of groundwater from northeastern part of Nagpur urban, Central India. *Environmental Earth Sciences*, 62(7), 1419–1430.
- McLean, W., Jankowski, J., & Lavitt, N. (2000). Groundwater quality and sustainability in an alluvial aquifer, Australia. In *Groundwater, past achievements and future challenges: A Balkema, Rotterdam*, pp. 567–573.
- Meybeck, M. (2003). Global analysis of river systems: From earth system controls to Anthropocene controls. *Philosophical Transactions of Royal Academy of London B*, 358(1440), 1935–1955.
- Miri, M., Bhatnagar, A., Mahdavi, Y., Basiri, L., Nakhaei, A., Khosravi, R., et al. (2018). Probabilistic risk assessment of exposure to fluoride in most consumed brands of tea in the Middle East. *Food and Chemical Toxicology*, 115, 267–272.
- Misra, A. K., & Mishra, A. (2007). Study of quaternary aquifers in Ganga Plain, India: focus on groundwater salinity, fluoride and fluorosis. *Journal of Hazardous Materials*, 144(1–2), 438–448.
- Mizan, S. A., Chatterjee, A., & Ahmed, S. (2017). Arsenic enrichment in groundwater in southern flood plain of Ganga-Son interfluvies. *Arabian Journal of Geosciences*, 10(5), 100.
- Njitchoua, R., Dever, L., Fontes, J. C., & Naah, E. (1997). Geochemistry, origin and recharge mechanisms of groundwaters from the Garoua Sandstone aquifer, northern Cameroon. *Journal of Hydrology*, 190(1–2), 123–140.
- Omo-Irabor, O. O., Olobaniyi, S. B., Oduyemi, K., & Akunna, J. (2008). Surface and groundwater water quality assessment using multivariate analytical methods: A case study of the Western Niger Delta, Nigeria. *Physics and Chemistry of the Earth, Parts A/B/C*, 33(8–13), 666–673.
- Pacheco, F. A. L., & Szocs, T. (2006). “Dedolomitization Reactions” driven by anthropogenic activity on loessy Sediments, SW Hungary. *Applied Geochemistry*, 21, 614–631.
- Pandey, S. K., Singh, A. K., & Hasnain, S. I. (2001). Hydrochemical characteristics of meltwater draining from Pindari glacier, Kumon Himalaya. *Journal of the Geological Society of India*, 57, 519–527.
- Patel, P., Raju, N. J., Reddy, B. S. R., Suresh, U., Gossel, W., & Wycisk, P. (2016). Geochemical processes and multivariate statistical analysis for the assessment of groundwater quality in the Swarnamukhi River basin, Andhra Pradesh, India. *Environmental Earth Sciences*, 75(7), 611.
- Pawar, N. J., & Pawar, J. B. (2016). Intra-annual variability in the heavy metal geochemistry of ground waters from the Deccan basaltic aquifers of India. *Environmental Earth Sciences*, 75(8), 654.
- Piper, A. M. (1944). A graphic procedure in the geochemical interpretation of water-analyses. *Eos, Transactions American Geophysical Union*, 25(6), 914–928.
- Postma, D., Boesen, C., Kristiansen, H., & Larsen, F. (1991). Nitrate reduction in an unconfined sandy aquifer: Water chemistry, reduction processes, and geochemical modeling. *Water Resources Research*, 27(8), 2027–2045.
- Qasemi, M., Farhang, M., Biglari, H., Afsharnia, M., Ojrati, A., Khani, F., et al. (2018). Health risk assessments due to nitrate levels in drinking water in villages of Azadshahr, northeastern Iran. *Environmental Earth Sciences*, 77(23), 782.
- Radfard, M., Yunesian, M., Nabizadeh, R., Biglari, H., Nazmara, S., Hadi, M., & Mahvi, A. H. (2018). Drinking water quality and arsenic health risk assessment in Sistan and Baluchestan, Southeastern Province, Iran. *Human and Ecological Risk Assessment: An International Journal*, pp. 1–17.
- Raja, G., & Venkatesan, P. (2010). Assessment of groundwater pollution and its impact in and around Punnam area of Karur District, Tamilnadu, India. *Journal of Chemistry*, 7(2), 473–478.
- Raju, N. J. (2012). Evaluation of hydrogeochemical processes in the Pleistocene aquifers of middle Ganga Plain, Uttar Pradesh, India. *Environmental Earth Sciences*, 65(4), 1291–1308.
- Raju, N. J., Patel, P., Reddy, B. S. R., Suresh, U., & Reddy, T. V. K. (2016). Identifying source and evaluation of hydrogeochemical processes in the hard rock aquifer system: Geostatistical analysis and geochemical modeling techniques. *Environmental Earth Sciences*, 75(16), 1157.
- Raju, N. J., Ram, P., & Dey, S. (2009). Groundwater quality in the lower Varuna river basin, Varanasi district, Uttar Pradesh. *Journal of the Geological Society of India*, 73(2), 178.
- Raju, N. J., Ram, P., & Gossel, W. (2014). Evaluation of groundwater vulnerability in the lower Varuna catchment area, Uttar Pradesh, India using AVI concept. *Journal of the Geological Society of India*, 83(3), 273–278.

- Raju, N. J., Shukla, U. K., & Ram, P. (2011). Hydrogeochemistry for the assessment of groundwater quality in Varanasi: A fast-urbanizing center in Uttar Pradesh, India. *Environmental Monitoring and Assessment*, 173(1–4), 279–300.
- Rao, N. S., Rao, J. P., Devadas, D. J., Rao, K. S., Krishna, C., & Rao, B. N. (2002). Hydrogeochemistry and groundwater quality in a developing urban environment of a semi-arid region, Guntur, Andhra Pradesh. *Journal of the Geological Society of India*, 59(2), 159–166.
- Richards, L. A. (1954). Diagnosis and improvement of saline and alkali soils. *Handbook*, 60.
- Sarin, M. M., Krishnaswami, S., Dilli, K., Somayajulu, B. L. K., & Moore, W. S. (1989). Major ion chemistry of the Ganga-Brahmaputra river system: Weathering processes and fluxes to the Bay of Bengal. *Geochimica et Cosmochimica Acta*, 53(5), 997–1009.
- Sawyer, C. N., & Mc Carty, P. L. (1967). Chemistry for Sanitary Engineers, and classification of naturally soft and naturally hard waters to sources and hardness of their water supplies. *Journal of Hygiene*.
- Schoeller, H. (1965). Qualitative evaluation of groundwater resources. In *Methods and techniques of groundwater investigations and development*. UNESCO, 5483.
- Schot, P. P., & Van der Wal, J. (1992). Human impact on regional groundwater composition through intervention in natural flow patterns and changes in land use. *Journal of Hydrology*, 134(1–4), 297–313.
- Shah, B. A. (2010). Arsenic-contaminated groundwater in Holocene sediments from parts of middle Ganga plain, Uttar Pradesh, India. *Current Science (Bangalore)*, 98(10), 1359–1365.
- Shukla, U. K., & Raju, N. J. (2008). Migration of the Ganga river and its implication on hydro-geological potential of Varanasi area, UP, India. *Journal of Earth System Science*, 117(4), 489–498.
- Singh, S., Raju, N. J., Gossel, W., & Wycisk, P. (2016). Assessment of pollution potential of leachate from the municipal solid waste disposal site and its impact on groundwater quality, Varanasi environs, India. *Arabian Journal of Geosciences*, 9(2), 131.
- Singh, A. K., Tewary, B. K., & Sinha, A. (2011). Hydrochemistry and quality assessment of groundwater in part of NOIDA metropolitan city, Uttar Pradesh. *Journal of the Geological Society of India*, 78(6), 523–540.
- Stadler, S., Talma, A. S., Tredoux, G., & Wrabel, J. (2012). Identification of sources and infiltration regimes of nitrate in the semi-arid Kalahari: Regional differences and implications for groundwater management. *Water SA*, 38(2), 213–224.
- Stumm, W., & Morgan, J. J. (1970). *Aquatic chemistry: An introduction emphasizing chemical equilibria in natural waters*.
- Thakur, D., Bartarya, S. K., & Nainwal, H. C. (2018). Groundwater quality assessment of the Soan Basin in Outer Himalaya, Himachal Pradesh, India. *Himalayan Geology*, 39(2), 197–211.
- Todd, D. K. (1980). Groundwater. In *Hydrology, 2nd Edition*. Wiley, p. 315
- US EPA (United State Environmental Protection Agency). (1986). Guidelines for the health risk assessment of chemical mixtures. *Federal Register*, 51(185), 34014–34025.
- US EPA (United State Environmental Protection Agency) (2000) Handbook for non cancer health effects evaluation. Washington, DC.
- Walker, R. (1990). Nitrates, nitrites and N-nitrosocompounds: A review of the occurrence in food and diet and the toxicological implications. *Food Additives & Contaminants*, 7(6), 717–768.
- Wilcox, L. V. (1948). *The quality of water for irrigation use* (No. 1488-2016-124600).
- Wolfe, A. H., & Patz, J. A. (2002). Reactive nitrogen and human health: acute and long-term implications. *Ambio: A Journal of the Human Environment*, 31(2), 120–126.
- World Health Organization. (1997). Guideline for drinking water quality, 2nd edn. WHO, Geneva, Health criteria and other supporting information, pp. 940–949.
- Wu, J., & Sun, Z. (2016). Evaluation of shallow groundwater contamination and associated human health risk in an alluvial plain impacted by agricultural and industrial activities, mid-west China. *Exposure and Health*, 8(3), 311–329.